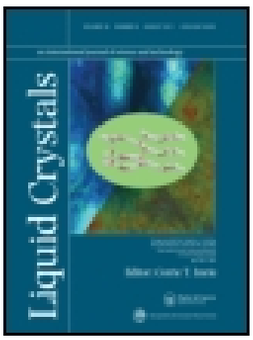

Liquid Crystals

ISSN: 0267-8292 (Print) 1366-5855 (Online) Journal homepage: https://www.tandfonline.com/loi/tlct20

Design and fabrication of 2 kHz nematic liquid crystal variable retarder with reflection mode

Zhaoliang Cao, Zenghui Peng, Li Xuan & Zhigang Zheng

To cite this article: Zhaoliang Cao, Zenghui Peng, Li Xuan & Zhigang Zheng (2019): Design and fabrication of 2 kHz nematic liquid crystal variable retarder with reflection mode, Liquid Crystals, DOI: 10.1080/02678292.2019.1686778

To link to this article: https://doi.org/10.1080/02678292.2019.1686778

Published online: 31 Oct 2019.

Submit your article to this journal

Article views: 19

View related articles

View Crossmark data

Full Terms & Conditions of access and use can be found at
https://www.tandfonline.com/action/journalInformation?journalCode=tlct20

LIQUID CRYSTALS
https://doi.org/10.1080/02678292.2019.1686778

Taylor & Francis
Taylor & Francis Group

Check for updates

Design and fabrication of 2 kHz nematic liquid crystal variable retarder with reflection mode

Zhaoliang Cao[a], Zenghui Peng[b], Li Xuan[b] and Zhigang Zheng[b,c]

[a]School of Mathematics and Physics, Suzhou University of Science and Technology, Suzhou, Jiangsu, China; [b]State Key Laboratory of Applied Optics, Changchun Institute of Optics, Fine Mechanics and Physics, Chinese Academy of Sciences, Changchun, Jilin, China; [c]Department of Physics, East China University of Science and Technology, Shanghai, China

ABSTRACT

This study proposes a simple method of designing a high-speed liquid crystal variable retarder (LCVR) with reflection mode. First, a series of simple formulas is provided for analysing the effects of tilt incidence and birefringence of the liquid crystal on the phase retardation and response time of the LCVR. Then, a reflective LCVR is fabricated to validate the theoretical analysis. Measured results show that the response speed can reach 2.7 kHz with a phase retardation of 1 λ. Furthermore, the theoretical curve is close to the measured curve while the incident angle is less than 10°. However, the theoretical and measured values show a considerable difference under a large incident angle. This problem is discussed, and a modified method is given. This work is helpful for the design and fabrication of high-speed LCVR.

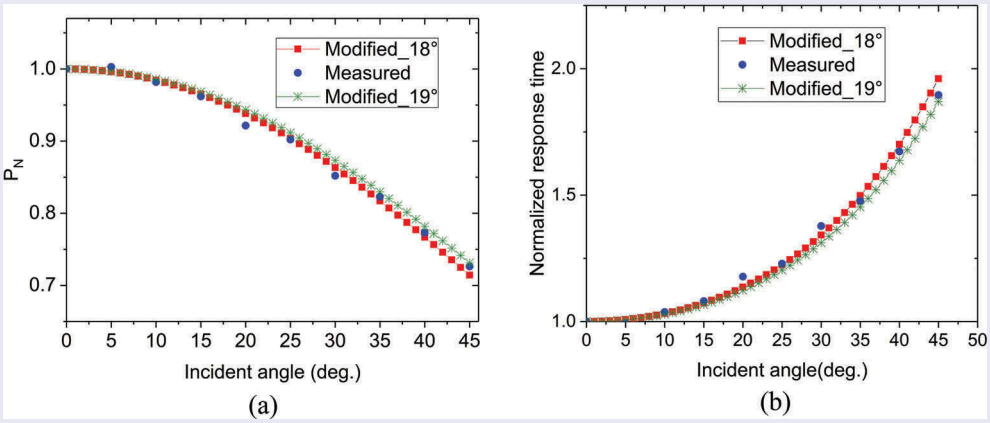

ARTICLE HISTORY
Received 14 September 2019
Accepted 27 October 2019

KEYWORDS
Variable retarder; reflection; tilt incidence; high speed

1 Introduction

Phase retarders are widely used in optical systems to retard the optical phase [1–4]. Phase retardation may be tuned in real time; tunable phase retarders, such as optical isolators [5,6], optical switches [7], and Q-switches [8,9], have been utilised in many optical systems and optical devices to simplify the configurations of optical systems. In particular, liquid crystal variable retarders (LCVRs) are researched extensively for their advantages of low power consumption, compact size, and low voltage [10–12]. With the development of technology, high-speed LCVRs are needed for many applications. For example, super-resolution structured illumination microscopy (SIM) [13,14] needs a tunable phase retarder to control the polarisation state of light. Given that SIM is used to observe biological phenomena, such as calcium sparks and the high-speed physiological response of organelles, it requires the transition rate of the polarisation state to be faster than the biological response. With the response time of these vital movements at the sub-millisecond order, the response time of LCVRs should be substantially less than 1 ms.

Researchers initially focused on improving the frame rate of liquid crystal spatial light modulators (LC SLMs) for adaptive wavefront correction. First, dual-frequency and ferroelectric liquid crystal (LC) materials were utilised to improve switching frequency, which can reach approximately 1 kHz [15–17]. However, such materials have many shortcomings. Dual-frequency LC SLMs

CONTACT Zhaoliang Cao caozl@usts.edu.cn; Zhigang Zheng zgzheng@ecust.edu.cn

© 2019 Informa UK Limited, trading as Taylor & Francis Group

need high driving voltages and complicated control methods, while ferroelectric LC SLMs have the drawbacks of binary phase modulation, fabrication difficulties, and small phase retardation.

Recently, nematic LC materials have been investigated to improve the response characteristic; the response time for LCs on silicon devices has decreased to less than 1 ms [18,19] at a wavelength of 785 nm. However, LCVRs are still fabricated normally using the transmission mode [2–4,10–12]. Compared with the response time of reflective LC SLMs, that of LCVRs is higher by approximately four times. Therefore, the reflection mode is considered in the current study to obtain high-frequency LCVRs. A beam splitter (BS) should be utilised to split the incident and reflected beams, whereas the LCVR is used with normal incidence because the reflection mode is adopted. Accordingly, the light energy will be decreased by 75%, which cannot be permitted for most optical systems. Tilt incidence may be selected to split the incident and reflected beams and thus avoid this problem. Consequently, this work mainly analyzes the effects of the birefringence Δn of LC and the incident angle on the phase retardation and response time of a reflective LCVR. Then, a series of simple equations is provided to approximately design the parameters of the LCVR. Finally, a reflective LCVR is fabricated and tested to validate the theoretical analysis.

2 Phase retardation of the reflective LCVR

2.1 Simplified model

A simplified configuration of the reflective LCVR is shown in Figure 1. The LC molecules are aligned in the horizontal direction. The cell thickness is d, and the incident angle is θ, which also represents the angle between the LC director and the electric field vector $\vec{E}$. In the model, the boarder effect is neglected, and all the LC molecules have the same tilt angle.

2.2 Analysis of normalised phase retardation

LC materials are uniaxial birefringence materials that have an ordinary refractive index n_o and an extraordinary refractive index n_e. For tilt incidence, $n_e(\theta)$ may be expressed with the refractive index ellipsoid equation [20] below:

$$n_e(\theta) = \frac{n_o n_e}{(n_o^2 \cos^2\theta + n_e^2 \sin^2\theta)^{1/2}}. \quad (1)$$

Therefore, given the change in the transmission distance of light, the phase retardation of tilt incidence with off-state may be calculated by

$$P_{tilt} = \frac{4\pi(n_e(\theta) - n_o)d}{\lambda \cos\theta}, \quad (2)$$

where λ is the related wavelength. With the assumption that the pretilt angle of the LC molecule is θ_0, Equation (2) can be rewritten as

$$P_{tilt} = \frac{2\pi d(n_e(\theta + \theta_0) + n_e(\theta - \theta_0) - 2n_o)}{\lambda \cos\theta}. \quad (3)$$

The response speed is fastest at normal incidence. Thus, in designing a reflective LCVR with tilt incidence, we expect the designed phase retardation to approach that of normal incidence. Moreover, the decrease magnitude of the phase retardation must be considered at a certain incident angle with the comparison of normal incidence. For quantification, a normalised phase retardation is defined as

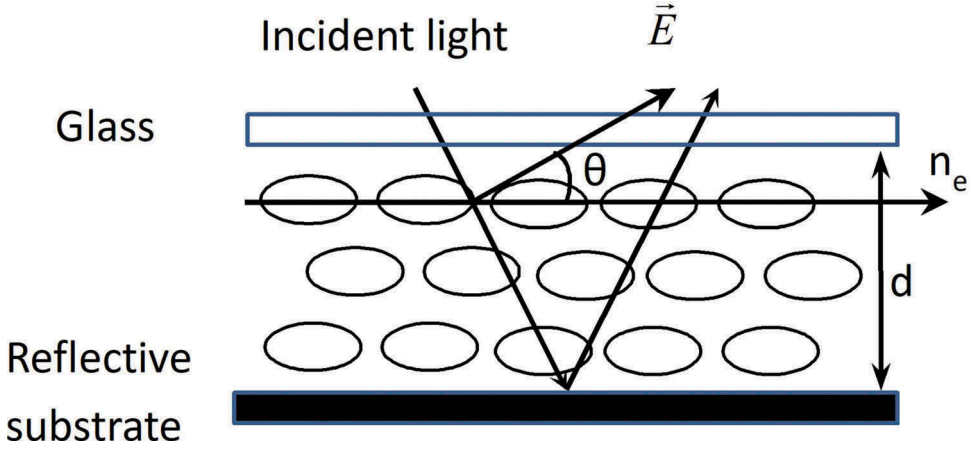

Figure 1. (Colour online) Structural model of reflective LCVR.

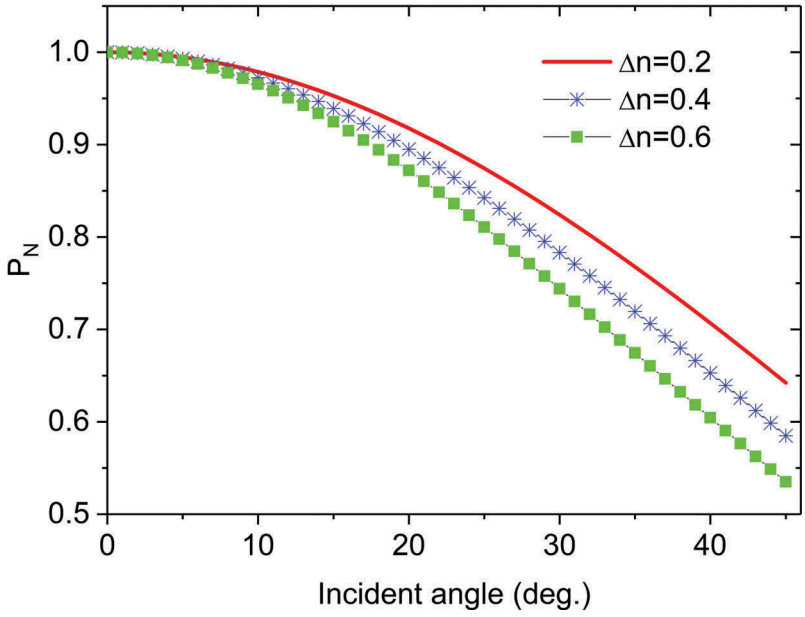

Figure 2. (Colour online) P_N as a function of incident angle with Δn=0.2, 0.4, 0.6.

$$P_N = \frac{P_{tilt}}{P_0} = \frac{(n_e(\theta+\theta_0)+n_e(\theta-\theta_0)-2n_o)}{2(n_e(\theta_0)-n_o)\cos\theta}, \quad (4)$$

where P_0 is the phase retardation at normal incidence and is expressed as

$$P_0 = \frac{4\pi d(n_e(\theta_0)-n_o)}{\lambda}. \quad (5)$$

Thus, the effect of tilt incidence on the phase retardation may be described with P_N. A large P_N indicates a small effect of tilt incidence. Equation (4) shows that the normalised phase retardation P_N has no relation with d and λ but is related to the birefringence Δn and the incident and pretilt angles θ and θ_0, respectively. In Figure 2, the normalised phase retardation is calculated as a function of the incident angle under $\theta_0 = 2°$, $n_o = 1.5$, $n_e = 1.7$, 1.9, and 2.1. P_N decreases slowly while the incident angle is less than 10°. However, P_N reduces drastically as the incident angle increases further. For the incident angles 15° and 45° with $\Delta n = 0.6$, the P_N values are 0.93 and 0.535, respectively. These values mean that phase retardation decreases by 7% and 46.5%, respectively. Therefore, the incident angle must be considered for the design of the LCVR.

The effect of birefringence on P_N is also analysed under $n_o = 1.5$, $\theta_0 = 2°$, $\theta = 15°$, 30°, and 45°. As shown in Figure 3, P_N reduces linearly, and a large incident angle causes a big variation in the normalised phase retardation as n_e changes from 1.6 to 2.1. The variations of P_N to $\theta = 15°$, 30°, and 45° are 0.035, 0.1, and 0.14, respectively, while Δn changes from 0.1 to 0.6. Consequently, the effect of birefringence should also be considered for the design of the LCVR.

Finally, the effect of pretilt angle is also considered. The pretilt angle of LC devices is normally at approximately 1°–5°, and we use this angle to perform the simulation. The relation between normalised phase retardation and pretilt angle with $\theta = 45°$ and $\Delta n = 0.6$ is computed in Figure 4. P_N increases while the pretilt angle changes from 1° to 5°. As P_N varies by only 0.011, it may be ignored in the LCVR design. Therefore, in this work, the incident angle of 2° is used to perform the computation. Our calculated results are similar to that in Refs [21–23]. for the effect of pretilt angle. It illustrates that the proposed computation method is effective. Figure 5 shows P_N as a function of the birefringence and incident angle, which can be used to design the phase retardation of the reflective LCVR.

3 Response time of reflective LCVR

The response time of LC devices includes the rise and decay times, with the former typically smaller than the latter. Consequently, the response speed is determined by the decay time [24] as

$$\tau_{decay} = \frac{\gamma_1 d^2}{K_{11}\pi^2}, \quad (6)$$

where γ_1 and K_{11} are the rotational viscosity coefficient and splay elastic constant of the LC, respectively. The fast response characteristic of LCVR may be acquired by decreasing the viscosity γ_1 and the cell thickness d. The

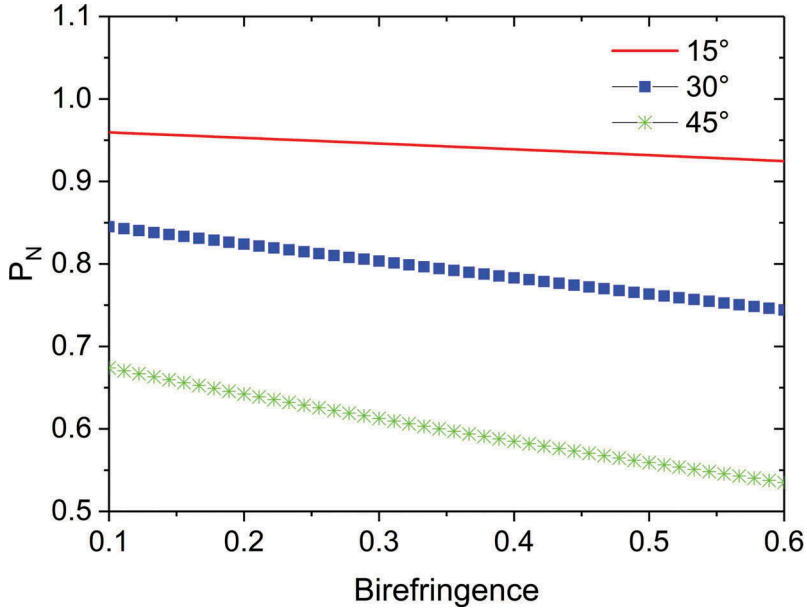

Figure 3. (Colour online) P_N as a function of Δn with incident angles 15°, 30°, and 45°.

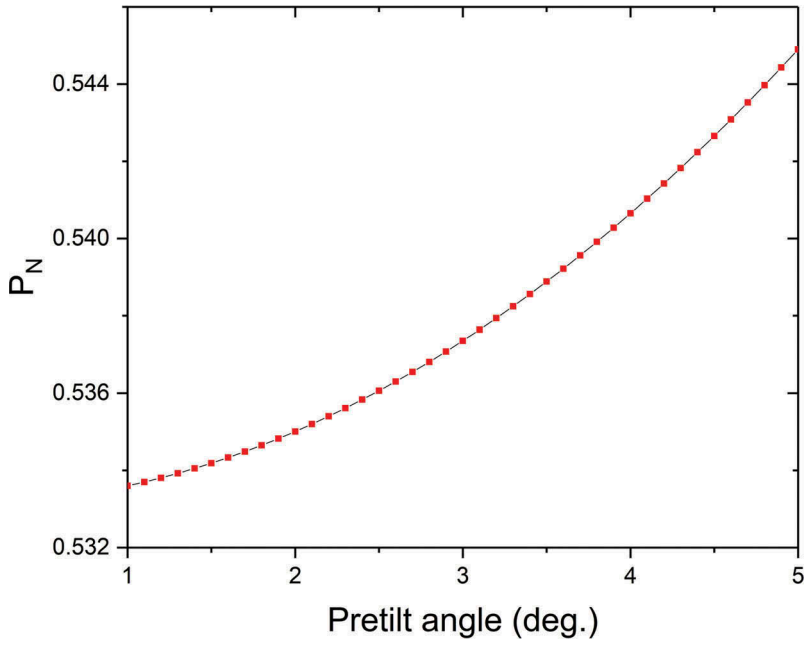

Figure 4. (Colour online) P_N as function of pretilt angle.

dynamic switch of LCVR has been considered in many papers [25–27]. The current study only considers the effect of cell thickness on the response time at tilt incidence.

With the assumption that the designed value of phase retardation is P, the cell thickness of the reflective LCVR to normal incidence is

$$d_0 = \frac{P\lambda}{4\pi\Delta n} = \frac{P\lambda}{4\pi(n_e(\theta_0) - n_o)}. \quad (7)$$

For tilt incidence, the cell thickness may be calculated to obtain the same phase retardation P by

$$d_{tilt} = \frac{P\lambda\cos\theta}{2\pi(n_e(\theta+\theta_0) + n_e(\theta-\theta_0) - 2n_o)}. \quad (8)$$

To evaluate the effect of tilt incidence on the response time, a normalised cell thickness is defined as

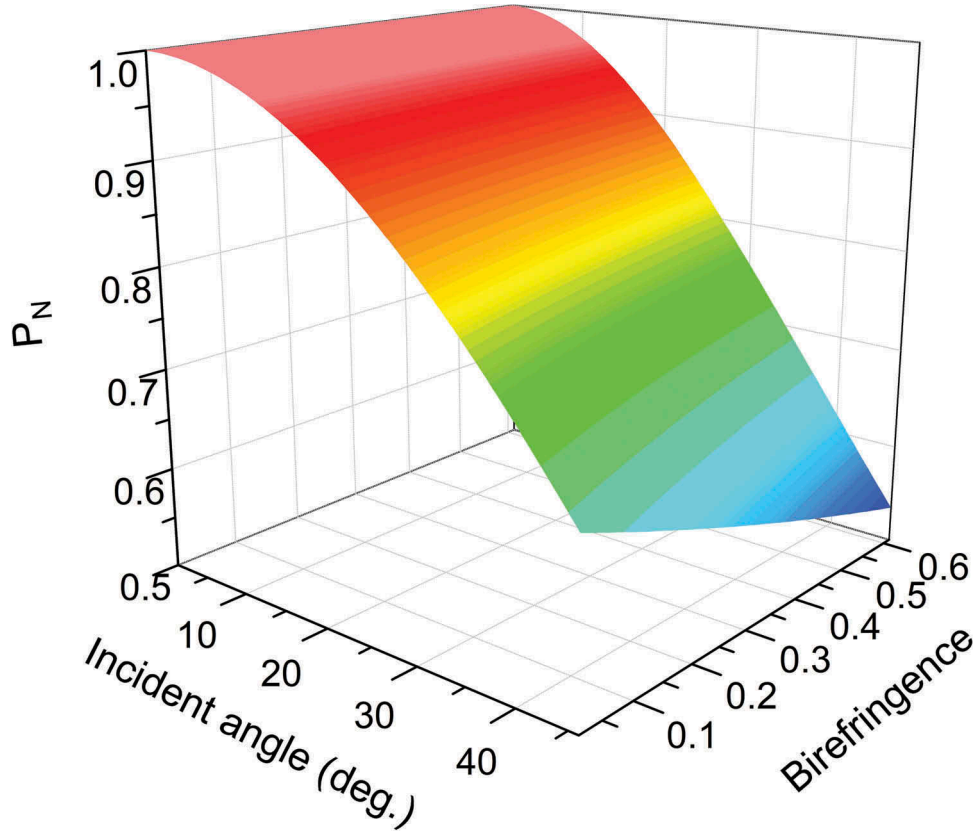

Figure 5. (Colour online) P_N as a function of incident angle and Δn.

$$d_N = \frac{d_{tilt}}{d_0} = \frac{2(n_e(\theta_0) - n_o)\cos\theta}{(n_e(\theta + \theta_0) + n_e(\theta - \theta_0) - 2n_o)}. \quad (9)$$

Equation (6) shows that the response time is proportional to the square of d. Thus, the normalised response time may be written as

$$\tau_N = \frac{\tau_{tilt}}{\tau_0} = \left(\frac{d_{tilt}}{d_0}\right)^2 = d_N^2, \quad (10)$$

where τ_0 and τ_{tilt} are the response times of the normal and tilt incidences, respectively. Equations (9) and (10) show that the normalised response time is related to the birefringence, incident angle, and pretilt angle. Furthermore, by comparing Equation (4) with Equations (9) and (10), we can acquire the following relation:

$$\tau_N = d_N^2 = \frac{1}{P_N^2}. \quad (11)$$

Hence, the normalised response time can be achieved accordingly with the known normalised phase retardation to design the reflective LCVR.

The effect of incident angle is calculated with $n_o = 1.5$, $\theta_0 = 2°$, $n_e = 1.7$, 1.9, and 2.1 in accordance with Equations (9) and (10), and the results are shown in Figure 6. The ratio between the response times of the transmitted and reflective LCVRs with normal incidence is also given for comparison. The incident angle is less than 10°; the effect of the incident angle and birefringence are considerably small, and the maximum normalised response time is 1.07 only. τ_N increases greatly when the incident angle exceeds 20°. However, τ_N remains less than R_{trans} even at an incident angle of 45°. Therefore, the response time of LCVR can be reduced substantially with the reflection mode.

The effect of birefringence is also considered under $\theta_0 = 2°$, $\theta = 15°$, 30°, and 45°, and the results are shown in Figure 7. The normalised response time is enlarged linearly with increased birefringence. For the incident angle of 15°, the effect of Δn is small, and the maximum normalised response time is merely 1.2. However, the effect of Δn increases with the incident angle. For example, for the incident angle of 45°, the normalised response time changes from 2.2 to 3.5 as the birefringence changes from 0.1 to 0.6. Figure 8 shows the normalised response time as a function of the incident angle and birefringence. Thus, the incident angle affects the normalised response time severely even with a small birefringence. The optimal incident angle and birefringence may be selected in accordance with the computed results in Figure 8.

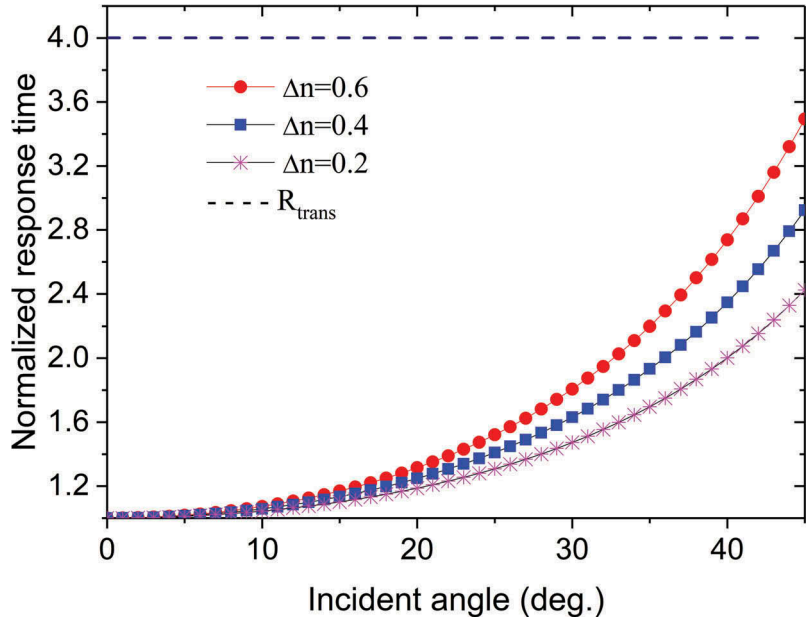

Figure 6. (Colour online) Normalized response time as function of incident angle with Δn =0.2, 0.4, 0.6.

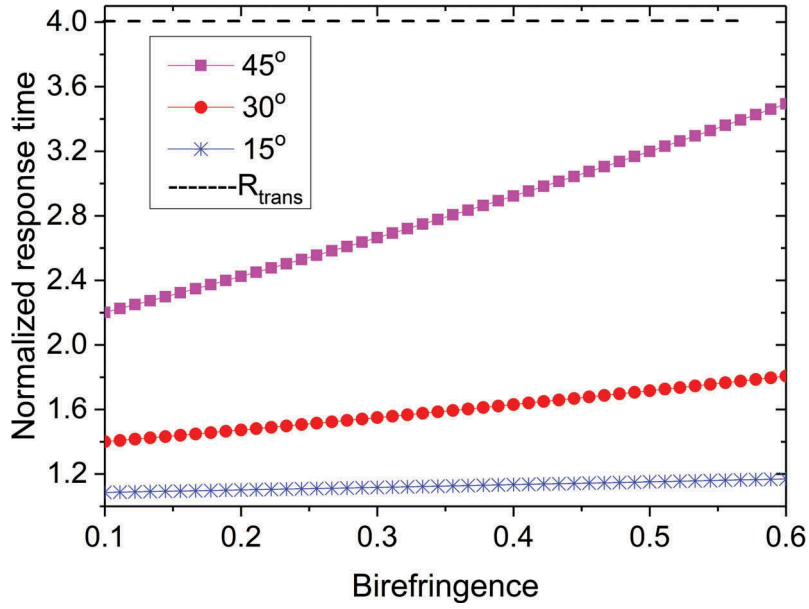

Figure 7. (Colour online) Normalized response time as function of Δn with incident angles 15°, 30°, and 45°.

4 Experiment

4.1 Design and fabrication of reflective LCVR

To evaluate the validity of the theoretical analysis, a reflective LCVR is designed for an SIM with the required parameters of $\lambda = 651$ nm, maximum phase retardation 1 λ, and response time of less than 0.5 ms. The synthetised LC material is used with the parameters $\Delta n = 0.44$, $\gamma_1 = 60$ cP, and $K_{11} = 2 \times 10^{-11}$ N/m to obtain a high-speed LCVR. The overdriving technique is adopted to achieve a fast response, and 1.5 λ phase retardation is demanded to acquire the optimal response characteristic [28,29]. Moreover, the PI alignment layer with the pretilt angle of 2° is chosen to align the LC molecule. Thus, the cell thickness may be calculated with Equation (7), and its value is 1.2 μm. The response time of the reflective LCVR with normal incidence is computed with Equation (6) to be 0.44 ms. Tilt incidence is utilised to split the incident and reflected beams. The computed results show normalised and actual response times of 1.13 and 0.5 ms, respectively, at the incident angle of 15°. Furthermore, the calculated P_N is 0.94, and the phase retardation is 1.4 λ; these results satisfy the demand of the

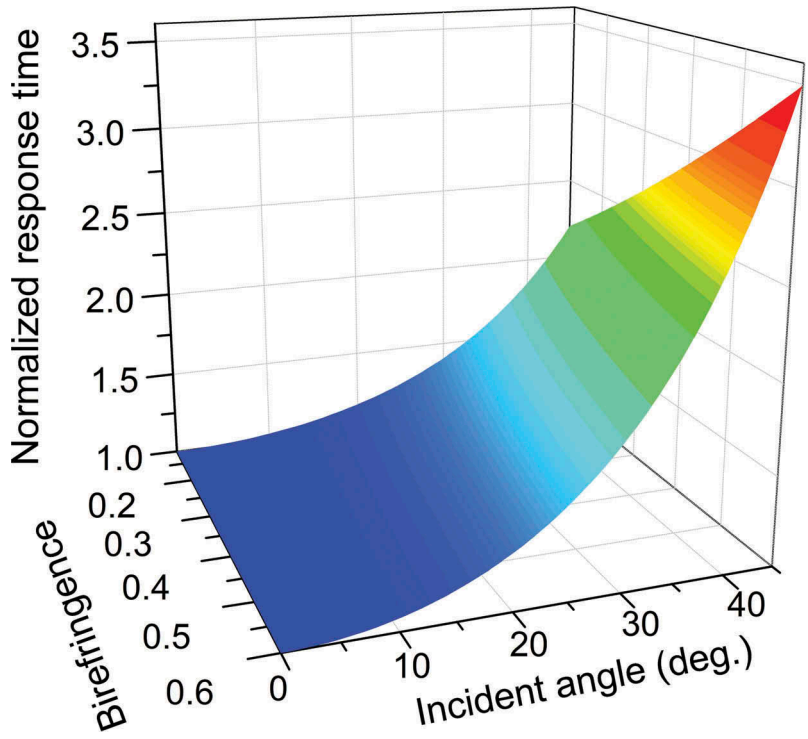

Figure 8. (Colour online) Normalized response time as function of Δn and incident angle.

overdriving technique. Therefore, the designed parameters are d= 1.2 μm, θ = 15°, θ_0 = 2°, and Δn = 0.44.

In practice, LC cells with a thickness of 1.2 μm cannot be easily fabricated. Hence, a reflective LCVR is created with a cell thickness of 2 μm, and the phase retardation of the normal incidence is 2.7 λ. In accordance with Equation (10), the response time will be increased 2.7 times, and the response time will be 1.35 ms, which cannot satisfy the design object. However, the overdriving technique can improve the response speed approximately four times. Consequently, the response time can remain under 0.5 ms with the overdriving technique.

4.2 Measurement

An optical testing system is established in a laboratory to measure the phase retardation and response time of the reflective LCVR (Figure 9). Light is emitted from a 651 nm laser, and its intensity may be tuned by an attenuator. Then, the beam is polarised by polarizer1 and reflected by the LCVR. The reflected light is transmitted via polarizer2 and enters a photodetector. The signal generator is used to apply the voltage onto the LCVR, and the change in the light intensity is recorded by an oscilloscope. A BS is used to measure the phase retardation of the LCVR at normal incidence. Polarizer2 and the photodetector should be moved to the area indicated by the dashed line. The phase change should be converted to intensity change to measure the phase retardation and the response time. For this purpose, the angle between the polarisation direction of polarizer1 and the alignment direction of the LC molecule should be 45°, and the polarisation direction of polarizer2 must be perpendicular to that of the polarizer1. Thus, the ordinary and extraordinary beams will interfere, and the phase change will be switched to the intensity variation accordingly. Finally, the phase change can be obtained with the recorded intensity data. The concrete measuring method is detailed in Ref [30].

A voltage of 5.5 V is applied on the LCVR to measure the phase retardation and response time. Then, the voltage is turned off, and the photodetector and the oscilloscope are used to receive and record the change in the intensity. The light intensity data are processed, and the phase retardation and response time are acquired. The measured response time with the designed incident angle of 15° is shown in Figure 10. The response time at the phase retardation of 1 λ is 0.37 ms, and the entire phase retardation is 2.34 λ. Thus, the response time of LCVR can be reduced to 0.37 ms, which corresponds to a frame rate of 2.7 kHz, by using the overdriving technique. Consequently, the fabricated reflective LCVR satisfies the designed parameters and may be used for the SIM.

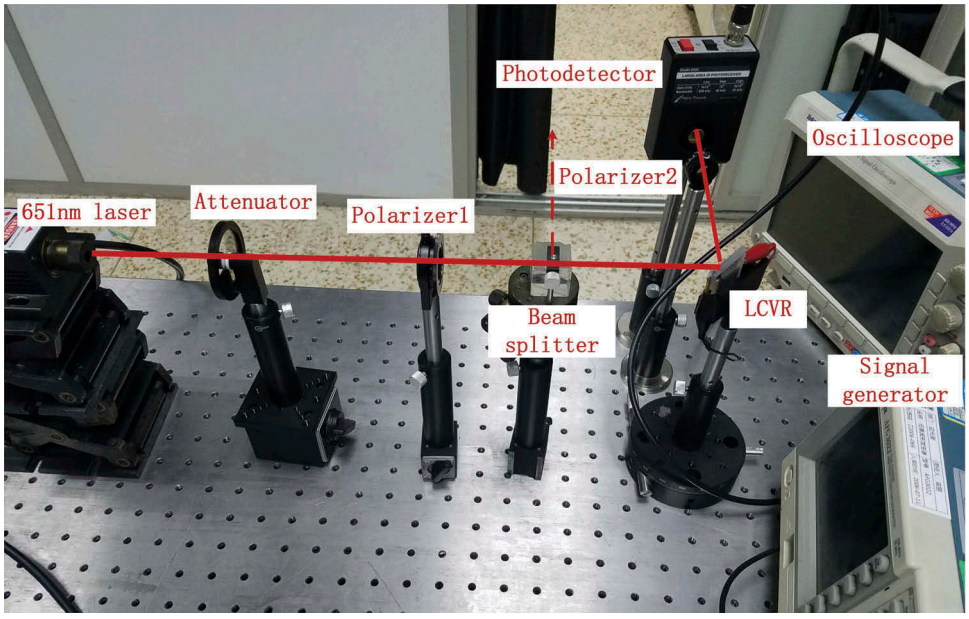

Figure 9. (Colour online) Optical setup for measuring reflective LCVR.

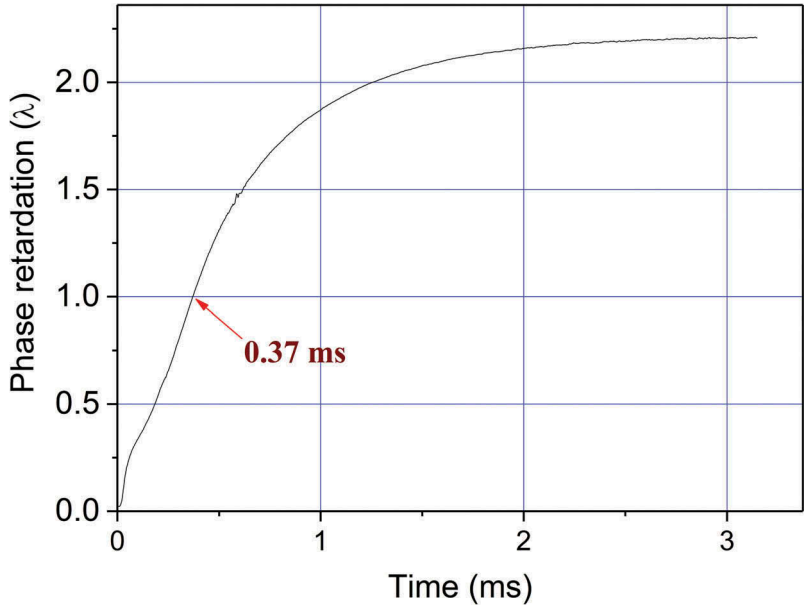

Figure 10. (Colour online) Phase retardation of LCVR as a function of response time.

The measured data are also normalised for comparison with the theoretical analysis findings, and the results are shown in Figures 11(a,b). The measured data are nearly the same as the theoretical results at incident angles less than 10°. However, the measured data increasingly deviate from the theoretical results as the incident angle increases from 10° to 45°. This problem is discussed in the next section.

5 Discussions

The theoretical and experimental results considerably differ at large incident angles. We believe that this discrepancy is caused by the difference between the theoretical driving voltage and that applied onto the LCVR in the experiment. In the theoretical model, an infinite voltage is applied, and the LC molecules are completely perpendicular to the substrate. The LC molecules

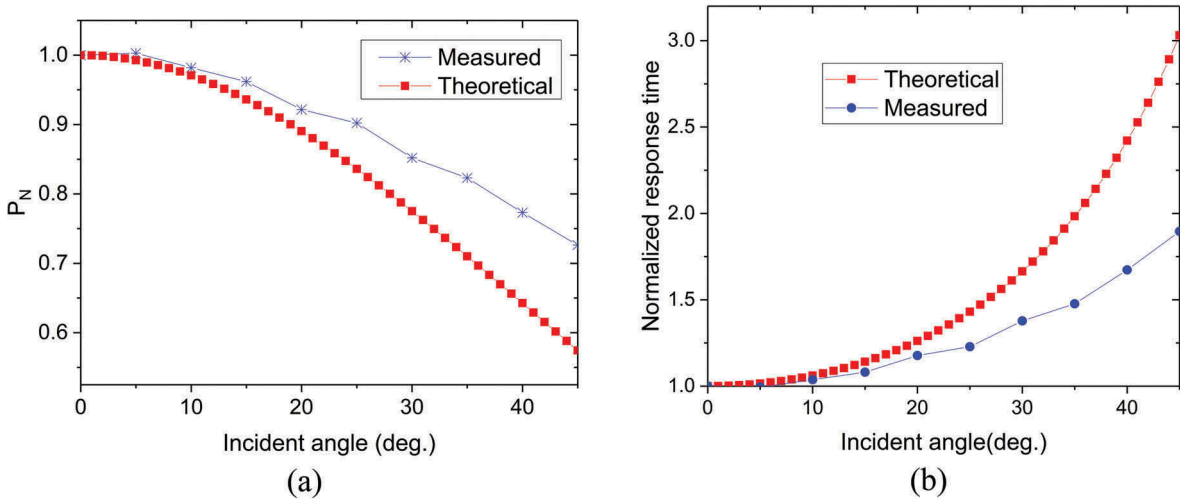

Figure 11. (Colour online) Normalized (a) phase retardation and (b) response time as functions of incident angle.

cannot stand fully because only a 5.5 V voltage is applied on the LCVR. Then the measured maximum phase retardation will be reduced. The maximum tilt angle of LC molecules at the centre of the cell, as a function of voltage, is used as follows to analyse the effect of the applied field [31]:

$$\varphi_{\mathrm{m}} = 2\sqrt{\left(\frac{U}{U_0} - 1\right)} \Big/ \sqrt{\left(1 + K + \left(\varepsilon_{\mathrm{p}} - \varepsilon_{\perp}\right)/\varepsilon_{\perp}\right)} \tag{12}$$

where U and U_0 are the applied and threshold voltages, respectively; $\varepsilon_{\parallel}$ and $\varepsilon_{\perp}$ are the permittivity at the parallel and perpendicular directions, respectively; and $K = (K_{33} - K_{11})/K_{11}$, where K_{11} and K_{33} are the splay and bend Frank elastic constants, respectively. The average tilt angle of the LC molecules may be calculated by [32]

$$\varphi_{ave} = 2\varphi_m/\pi. \tag{13}$$

Thus, the phase retardation of normal incidence with the applied field may be computed by

$$P_{Volt} = \frac{4\pi(n_e(\theta_0) - n_e(\varphi_{ave}))d}{\lambda}. \tag{14}$$

For the LC material used in the experiment, U_0 = 1.2 V, $K_{33} = 3 \times 10^{-11}$ N/m, $K_{11} = 2 \times 10^{-11}$ N/m, $\varepsilon_{\parallel}$ = 19.6, and $\varepsilon_{\perp}$ = 4.5. Thus, the phase retardation can be calculated as a function of the applied field in accordance with Equations (12)–(14), and the result is shown in Figure 12. The phase retardation at 5.5 V voltage is 2.3 λ, which is close to the measured value of 2.34 λ. Moreover, the curve tends to be constant when the voltage increases to 10 V. These findings illustrate that the phase retardation will have nearly no increase as the voltage further increases. When the voltage is 10 V, the phase retardation is 2.7 λ, which is equal to the designed value of normal incidence. These results indicate that the phase retardation change of the fabricated LCVR may be described by Equation (14). Therefore, Equations (12)–(14) may be used to estimate the effect of the applied field.

As shown in Figure 13(a), the LC molecules are rotated from zero to the angle ϕ_{ave} because of the effect of the applied field. The equivalent simplified model shown in Figure 13(b) is used to modify the theoretical formula conveniently by simulating the reduction of phase retardation and assuming that Figures 13(a,b) have the same phase retardation. Thus, the effect of the applied field is switched to the effect of the pretilt angle, and the effective pretilt angle should be acquired first to modify the effect of the applied field. The phase retardation P_{Volt} can be computed by Equation (14) with the known applied field. Thus, the effective pretilt angle may be calculated by Equation (5) under the condition of $P_{Volt} = P_0$. Then, the modified normalised phase retardation and response time may be obtained by substituting the effective pretilt angle into Equations (4) and (9), respectively.

In the experiment, the measured maximum phase retardation is 2.34 λ at normal incidence, and the corresponding effective pretilt angle is 18°. Furthermore, the phase retardation calculated with Equation (14) to the applied voltage of 5.5 V is 2.3 λ, and the corresponding effective pretilt angle is 19°. The modified theoretical results with the effective pretilt angles of 18° and 19° are computed with Equations (4) and (9), respectively, as shown in Figure 14. For comparison, the measured data are given in Figure 14. These findings indicate that the measured results are close to the modified theoretical

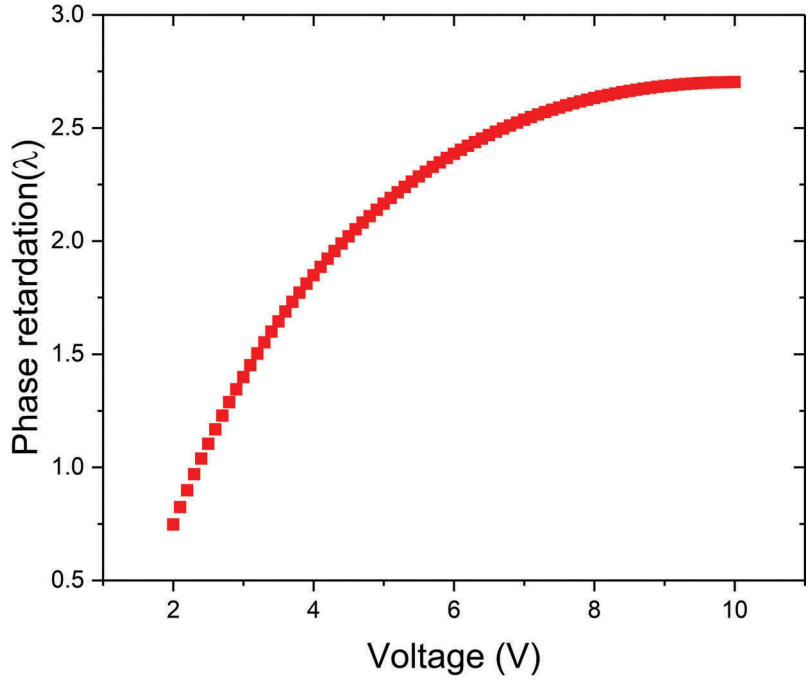

Figure 12. (Colour online) Phase retardation as a function of applied voltage.

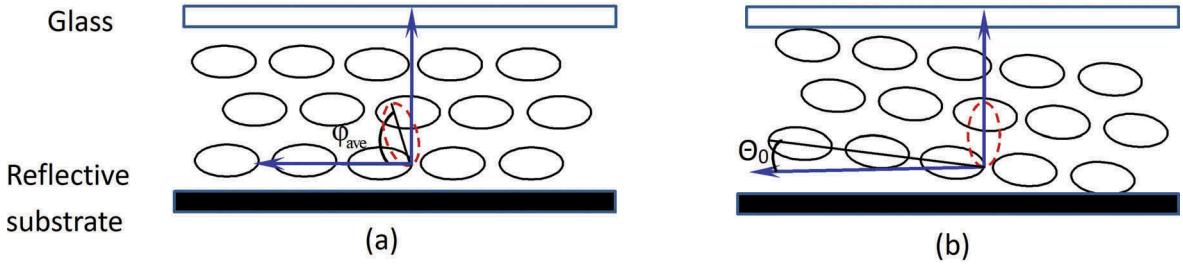

Figure 13. (Colour online) (a) Illustration of the effect of applied field on LC molecule rotation and (b) equivalent simplified model representing the effect of applied field.

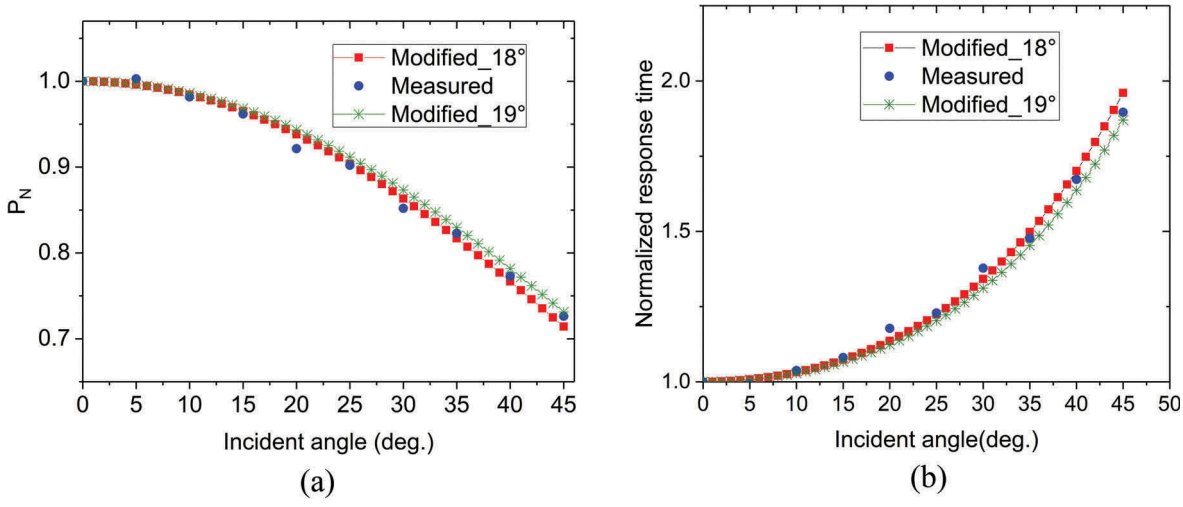

Figure 14. (Colour online) Modified theoretical and experimental results of reflective LCVR: (a) normalized phase retardation; (b) normalized response time.

data. Furthermore, both modified curves may be used to estimate the phase retardation and response time of the LCVR. Therefore, Equation (14) and the equivalent model may be utilised to modify the effect of the applied field. Furthermore, while the voltage is 10 V, the phase retardation is 2.7 λ, which equals the design value. The designed maximum phase retardation can be obtained with the 10 V voltage. Therefore, nearly all the LC molecules are stood completely and the effect of the applied field may be ignored. No modification needs to be operated. In summary, as the designed LCVR works at low voltages with large incident angles, the effect of the applied field should be considered, and the theoretical results should be modified accordingly.

6 Conclusions

A simple method is proposed for the design and fabrication of a high-speed reflective LCVR. First, a normalised phase retardation is defined to describe the phase change at tilt incidence compared with the phase retardation at normal incidence. Results indicate that the normalised phase retardation has no relation to the cell thickness and working wavelength, but it is related to the birefringence and the incident and pretilt angles. Then, the effects of tilt incidence, birefringence, and pretilt angle are analysed on the normalised phase retardation of the LCVR. Results show that the normalised phase retardation varies between 0.465 and 0.14, which correspond to an incident angle of 45° and a birefringence of 0.6. However, the normalised phase retardation only changes by 0.011 for the pretilt angle of 5°. Hence, the effect of pretilt angle may be ignored, but the effect of the incident angle and birefringence must be considered for the design of the reflective LCVR.

The effects of the birefringence and incident angle on the normalised response time are analysed as well. The theoretical analysis shows that the normalised response time is inversely proportional to the square of the normalised phase retardation. Moreover, when the incident angle is less than 10°, the effect of incident angle and birefringence are small, and the maximum normalised response time is only 1.07. However, an incident angle >10° affects the normalised response time severely even with a small birefringence. Consequently, the effects of incident angle and birefringence must be considered to achieve fast response.

A reflective LCVR is thus designed and fabricated to validate the theoretical computation method. The measured results for a wavelength of 651 nm and an incident angle of 15° show that the response speed can reach 2.7 kHz with a phase retardation of 1 λ, which matches the design object. Furthermore, the theoretical and measured curves considerably differ when the incident angle exceeds 10°. This problem is discussed, and the analysis findings show that it is caused by the difference between the theoretical assumption and the driving voltages applied onto the LCVR. Then, a simple formula is provided to compute the effects of the applied voltage, and an equivalent model is established to simulate the effect of the applied voltage. The effective pretilt angle may be calculated using this simple formula and its equivalent model. The theoretical computation can be modified by substituting the effective pretilt angle to these equations. The theoretical curve approximately coincides with the measured curve after the modification. Therefore, the theoretical model is effective, and the influence of the applied voltage must be considered in the design and fabrication of the LCVR, especially for applications with low voltages and large incident angles.

In conclusion, the established computation equations may be theoretically used to design high-speed reflective LCVRs. With this work, the frame rate of an LCVR can exceed 2 kHz, which is useful for applications that require high speeds, such as super-resolution SIM.

Disclosure statement

No potential conflict of interest was reported by the authors.

Funding

This work is supported by Jiangsu Key Disciplines of the Thirteenth Five-Year Plan (No. 20168765) and the State Key Laboratory of Applied Optics (No. M200-D-1716).

References

[1] Hu C, Xie P, Huo S, et al. A liquid crystal variable retarder-based reflectance difference spectrometer for fast, high precision spectroscopic measurements. Thin Solid Films. 2014;571:543–547.
[2] Watad I, Abdulhalim I. Phase-shifted polarimetric surface plasmon resonance sensor using a liquid crystal retarder and a diverging beam. Opt Lett. 2019;44:1607–1610.
[3] Yoshida S. Measurement of moving objects with phase-shifting digital holography using liquid crystal retarder. Opt Commun. 2018;420:141–146.
[4] August I, Oiknine Y, AbuLeil M, et al. Miniature compressive ultra-spectral imaging system utilizing a single liquid crystal phase retarder. Sci Rep. 2016;6:23524.
[5] Yamashita S, Okoshi T. Performance improvement and optimization of fiber amplifier with a midway isolator. IEEE Photonics Technol Lett. 1992;4:1276–1278.

[6] Ma X, Tao S. High-isolation optical isolator using a BiCaInVIG single crystal. Appl Opt. 1992;31:4122–4124.
[7] Ellis AD, Widdowson T, Shan X, et al. Three-node 40 Gb/s OTDM network experiment using electro-optic switches. Electron Lett. 1994;30:1333–1334.
[8] Honea EC, Beach RJ, Mitchell SC, et al. 183-W, M2=2.4 Yb: YAGQ-switched laser. Opt Lett. 1999;24:154–156.
[9] Carrig TJ, Wagner GJ, Sennaroglu A, et al. Mode-locked Cr2+: ZnSe laser. Opt Lett. 2000;25:168–170.
[10] Zhang Y, Xuan J, Zhao H, et al. Integrated spectral phase delay calibration technique for a liquid crystal variable retarder used in wide-bandwidth working channel. Opt Laser Technol. 2018;108:186–192.
[11] Bouchal P, Čelechovský R, Bouchal Z. Polarization sensitive phase-shifting Mirau interferometry using a liquid crystal variable retarder. Opt Lett. 2015;40:4567–4570.
[12] Jörg S, Theodor SK. Liquid crystal phase retarder with broad spectral range. Opt Commun. 2000;176:313–317.
[13] Kner P, Chhun BB, Griffis ER, et al. Super-resolution video microscopy of live cells by structured illumination. Nat Methods. 2009;6:339–342.
[14] Li D, Shao L, Chen BC, et al. Extended-resolution structured illumination imaging of endocytic and cytoskeletal dynamics. Science. 2015;349:aab3500.
[15] Gu D, Winker B, Wen B, et al. Wavefront control with a spatial light modulator containing dual frequency liquid crystal. Proc SPIE. 2004;5553:68–82.
[16] Burns DC, Underwood I, Gourlay J, et al. A 256 × 256 SRAM-XOR pixel ferroelectric liquid crystal over silicon spatial light modulator. Opt Commun. 1995;119:623–632.
[17] Serati S, Xia XW, Mughal O, et al. High-resolution phase-only spatial light modulators with sub millisecond response. Proc SPIE. 2003;5106:138–145.
[18] Peng Z, Wang Q, Liu Y, et al. Electrooptical properties of new type fluorinated phenyl-tolane isothiocyanate liquid crystal compounds. Liq Cryst. 2016;43:276–284.
[19] Peng ZH, Cao ZL, Yao LS, et al. The review of liquid crystal wavefront corrector with fast response property (in Chinese). Sci Sin-Phys Mech Astron. 2017;47:084203.
[20] Cao Z, Xuan L, Hu L, et al. Investigation of optical testing with a phase-only liquid crystal spatial light modulator. Opt Express. 2005;13:1059–1065.
[21] Belyaev VV, Solomatin AS, Chausov DN. Phase retardation vs. pretilt angle in liquid crystal cells with homogeneous and inhomogeneous LC director configuration. Opt Express. 2013;21:4244–4249.
[22] Belyaev VV, Solomatin AS, Chausov DN. Measurement of the liquid crystal pretilt angle in cells with homogeneous and inhomogeneous LC director configuration. Appl Opt. 2013;52:3012–3019.
[23] Belyaev VV, Solomatin AS, Chausov DN. Phase retardation difference of liquid crystal cells with symmetric and asymmetric boundary conditions. Mol Cryst Liq Cryst. 2014;596:22–29.
[24] Jakeman E, Raynes EP. Electro-optic response times in liquid crystals. Phys Lett A. 1972;39:69–70.
[25] Chigrinov VG, Belyaev VV. Time characteristics of orientational electrooptical effects in nematic liquid crystals. Sov Phys Crystallogr. 1977;22:344–346.
[26] Belyaev VV, Chigrinov VG. Dynamics of the twist effect in nematic liquid crystals: relaxation of angle of inclination of molecules. Sov Phys Crystallogr. 1978;23:614–616.
[27] Belyaev VV, Chigrinov VG. The switching dynamics of nematic liquid crystals with low-frequency dispersion of the dielectric anisotropy. Sov Phys Crystallogr. 1978;23:454–457.
[28] Yao L, Mu Q, Peng Z, et al. Optimising response of liquid crystal corrector with digital overdriving technique. Liq Cryst. 2013;40:817–821.
[29] Peng Z, Liu Y, Yao L, et al. Improvement of the switching frequency of a liquid-crystal spatial light modulator with optimal cell gap. Opt Lett. 2011;36:3608.
[30] Cao Z, Mu Q, Hu L, et al. Correction of horizontal turbulence with nematic liquid crystal wavefront corrector. Opt Express. 2008;16:7006–7013.
[31] 42nd Committee of Japan Society for the Promotion of Science. Liquid crystal device manual. Huang X, Huang H, Li Z, Translators. Beijing: Aviation industry press; 1992. p. 364.
[32] Sun Y, Zhang Z, Ma H. Optimal rubbing angle for reflective in-plane-switching liquid crystal displays. Appl Phys Lett. 2002;81:4907–4909.